Available online at www.sciencedirect.com
SCIENCE DIRECT®
Tetrahedron: Asymmetry
Tetrahedron: *Asymmetry* 15 (2004) 3079–3090

Enantiopure stereoisomeric homologues of glutamic acid: chemoenzymatic synthesis and assignment of their absolute configurations

Gabriella Roda,[a] Paola Conti,[a] Marco De Amici,[a,*] Jiangtao He,[b] Prasad L. Polavarapu[b,*] and Carlo De Micheli[a]

[a]*Istituto di Chimica Farmaceutica e Tossicologica, Università degli Studi di Milano, Viale Abruzzi 42, 20131 Milano, Italy*
[b]*Department of Chemistry, Vanderbilt University, Nashville, Tennessee 37235, USA*

Received 17 June 2004; accepted 16 July 2004

Abstract—The two enantiomeric pairs of bicyclic isoxazoline acidic amino acids, designed as conformationally constrained homologues of glutamic acid, have been prepared by taking advantage of a nitrile oxide cycloaddition coupled to highly selective biocatalyzed transformations. All four isomeric target amino acids were obtained with enantiomeric excesses higher than 99%. The absolute configurations were attributed to the compounds under study by comparing the experimental and theoretical vibrational circular dichroism features of two selected reaction intermediates. These absolute configurations were further confirmed using experimental and theoretical specific rotations.

1. Introduction

(*S*)-Glutamic acid **1** (Glu) (Fig. 1), the main excitatory neurotransmitter in the mammalian central nervous system, is involved in the physiological regulation of processes such as learning and memory.[1–3] On the other hand, glutamatergic hyperactivity leads to neurotoxicity typical of some acute and chronic neurodegenerative diseases, for example, cerebral ischemia, epilepsy, amyotrophic lateral sclerosis, Parkinson's, and Alzheimer's diseases.[1–3]

Glu acts at specific receptors belonging to two heterogeneous families: the ionotropic and the metabotropic glutamate receptors (iGluRs and mGluRs, respectively).[1–3] The fast excitatory effects of Glu are mediated by three subclasses of iGluRs, which are transmembrane cation channels named after their archetypal selective ligands, that is, *N*-methyl-D-aspartic acid **2** (NMDA), 2-amino-3-(3-hydroxy-5-methylisoxazol-4-yl)propionic acid **3** (AMPA), and kainic acid **4** (KA) (Fig. 1).[4,5] Conversely, the mGluRs are G-protein-coupled receptors, whose activation produces metabolic changes in the postsynaptic cells, owing to the stimulation/inhibition of the formation of second messengers. So far, eight subtypes of mGluRs have been cloned[6] and, later on, classified into three groups (I–III) according to their sequence homology, coupling with the second messenger and pharmacology.

The modulation of the glutamatergic pathways may represent a relevant therapeutic approach for the treatment of a number of neurodegenerative pathologies and neuropsychiatric diseases, as well as learning and memory impairments. Hence, novel high affinity ligands endowed with family and subtype selectivity are required to better characterize the physio-pathological role of iGluRs and mGluRs and, consequently, to uncover specific targets for pharmacological intervention. As an example, the potential therapeutic utility of NMDA antagonists in the treatment of cerebral ischemia and other neurodegenerative disorders has been recognized.[7,8] Unfortunately, competitive as well as noncompetitive NMDA antagonists tested in clinical trials showed severe adverse effects in humans, such as psychotomimetic and cardiovascular side effects.[9,10] On the other hand, it has been suggested that both group I antagonists as well as group II and III agonists

* Corresponding authors. Tel.: +39 02503 17555; fax: +39 02503 17565 (M.D.A.); tel.: +1 615 322 2836; fax: +1 615 322 4936 (P.L.P.); e-mail addresses: marco.deamici@unimi.it; prasad.l.polavarapu@vanderbilt.edu

0957-4166/$ - see front matter © 2004 Elsevier Ltd. All rights reserved.
doi:10.1016/j.tetasy.2004.07.037

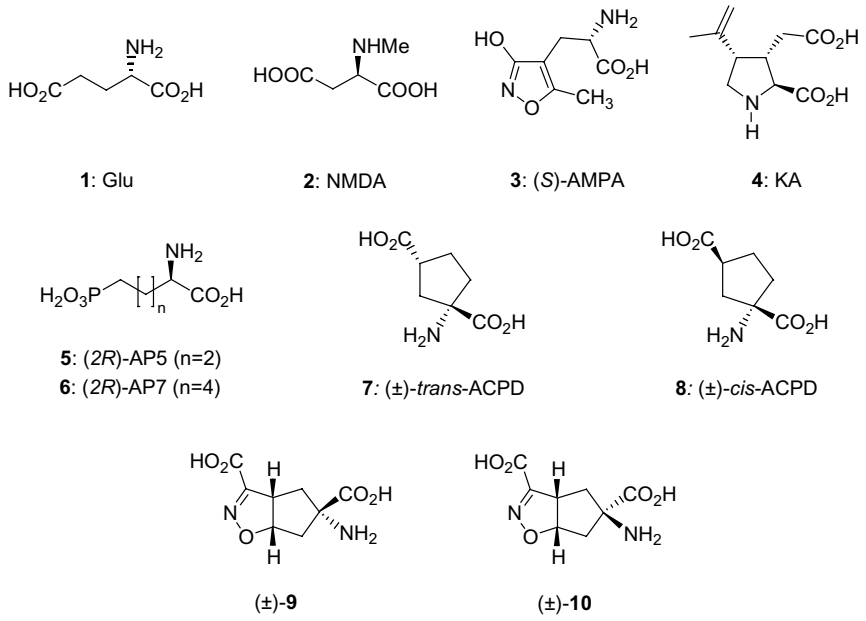

Figure 1. Structures of the reference and investigated ligands of the glutamate receptors.

may represent potentially useful tools for neuroprotection.[11,12]

As far as the interaction of ligands with NMDA receptors[13] is taken into account, an increase of the distance between the proximal and the distal acidic groups of Glu usually leads to NMDA antagonists, with the most potent NMDA antagonists bearing a chain of four or six carbon atoms linking the two acidic groups, that is, (2*R*)-2-amino-5-phosphonopentanoic acid **5** [(2*R*)-AP5] and (2*R*)-2-amino-7-phosphonoeptanoic acid **6** [(2*R*)-AP7] (Fig. 1). Remarkably, the eutomer of the majority of NMDA ligands has an absolute configuration at the amino acidic stereogenic center opposite to that of natural Glu, the endogenous neurotransmitter.[14]

The conformational profile of NMDA antagonists as well as mGluRs ligands has been the subject of intensive investigations. The results obtained on a number of rigidified amino acids, whose conformation has been constrained into cyclic structures, indicate that the majority of NMDA antagonists usually adopt a folded conformation, with the proximal and the distal acidic functionalities orientated toward the same face of the molecule.[13,15] On the other hand, it was ascertained that Glu binds to the different types of mGluRs in a fully extended conformation, that is, the conformation reproduced by (±)-*trans*-1-aminocyclopentane-1,3-dicarboxylic acid **7** (*trans*-ACPD) (Fig. 1), an unselective mGluRs agonist usually taken as a reference compound.[16] The pharmacological profile of **7** changes by simply reversing the spatial arrangement of the two acidic groups: in fact, (±)-*cis*-1-aminocyclopentane-1,3-dicarboxylic acid **8** (*cis*-ACPD) (Fig. 1) behaves as a group II mGluRs preferring agonist.[16]

In the search for new subtype selective ligands at the different glutamate receptors, we designed a group of 3-carboxy-Δ^2-isoxazoline acidic amino acids as new conformationally constrained analogues (or homologues) of Glu.[17–19]

In a recent report, we prepared and tested the two stereoisomeric homologues of Glu (±)-**9** and (±)-**10** with the amino acidic chain embedded in a bicyclic ring system.[20] When assayed at mGluRs, both amino acids behaved as antagonists at mGluR1,5 and as agonists at mGluR2. On the other hand, (±)-**9** was inactive at all iGluRs, whereas (±)-**10** displayed a quite potent antagonism at the NMDA receptors. The synergistic activity of (±)-**10** at NMDA and mGlu receptors suggests it as a new lead of neuroprotective agents. When tested in vivo on DBA/2 mice, both amino acids displayed a noteworthy anticonvulsant activity. Based on the above reported results, we planned the synthesis of the two enantiomers of (±)-**9** and (±)-**10**. The evaluation of the pharmacological profile of individual isomers would be of particular significance for (±)-**10**, since usually NMDA and mGlu receptors accommodate in their binding sites ligands with an opposite absolute configuration at the amino acidic stereogenic centers.

Herein the synthesis of the two pairs of enantiomers of 5-amino-4,5,6,6a-tetrahydro-3a*H*-cyclopenta[*d*]isoxazole-3,5-dicarboxylic acids (+)-**9**/(−)-**9** and (+)-**10**/(−)-**10** and the assignment of the absolute configurations to their stereogenic centers are detailed. The target amino acids were prepared in very high enantiomeric purity by enzyme-catalyzed bioconversion processes carried out on appropriate racemic substrates. In this respect, this paper represents an extension of similar approaches applied by our research group to the production of enantiopure chiral compounds of interest to medicinal chemistry.[21–23] Configurational assignments were accomplished by comparing the experimental and theoretical vibrational circular dichroism (VCD) spectra of two selected intermediates in the sequence of steps leading to the desired final compounds. These absolute

configurations were further confirmed using experimental and theoretical specific rotations.

2. Results and discussion

2.1. Chemistry

As depicted in Scheme 1, cycloadducts (±)-**12**, and (±)-**13** were prepared by reacting ethoxycarbonylformonitrile oxide, generated in situ by treatment of ethyl 2-chloro-2-(hydroxyimino)acetate with sodium bicarbonate, to a suitably protected 1-amino-cyclopent-3-enecarboxylic acid. In contrast to a previous report,[20] we chose to perform the pericyclic reaction with methyl *N*-(*tert*-butoxycarbonyl)-1-amino-cyclopent-3-enecarboxylate **11**,[24] in order to differentiate the two ester functions appended at positions 3 and 5 of the bicyclic system. Such an expedient was introduced to facilitate the evaluation of the outcome of the subsequent enzyme-catalyzed hydrolyses. As previously reported,[20] the observed diastereofacial selectivity is dictated by a transition state, which is stabilized by an intermolecular hydrogen bond between the NHBOC group of the dipolarophile and the negatively charged oxygen atom of the 1,3-dipole. The two cycloadducts (±)-**12** and (±)-**13** were separated by column chromatography and their relative configuration assigned by the chemical correlation with amino acids (±)-**9** and (±)-**10**, whose structures had been previously attributed.[20]

Diester (±)-**12** was submitted to hydrolysis under the catalysis of two lipases [lipase B from *Candida antarctica* (CALB) and lipase from *Pseudomonas cepacia* (lipase PS)] and one protease (chymotrypsin). Initially, the reactions were performed on an analytical scale at buffered pH with acetone as a co-solvent. The degree of conversion and the enantiomeric excess (ee) were determined by chiral HPLC analysis (Chiralcel OD-H, see Section 4), which gave base-line separations of the enantiomers of both residual diester **12** and monoacid **14**. Among the tested enzymes, CALB behaved as a highly selective catalyst, able to efficiently hydrolyze the ethyl ester function of (−)-**12** to the corresponding monoacid (−)-**14** (Scheme 1). It is noteworthy that the reaction spontaneously stopped at 50% conversion to yield monoacid (−)-**14** and residual ester (+)-**12** in ee's higher than 99%. The value of the enantiomeric ratio (E >500), calculated according to the literature,[25] is a measure of the high enantioselection observed. The absolute configuration of the single isomers, reported in Scheme 1, was assigned by a combination of experimental and theoretical analyses and will be discussed in the next section. The same hydrolysis carried out with lipase PS proceeded slowly, whereas the presence of chymotrypsin left the substrate unaffected. As a consequence, for preparative purposes, we used the regio- and enantioselective hydrolysis of diester (±)-**12** mediated by CALB.

Based on the above discussed results, we initially attempted the kinetic resolution of the minor stereoisomer (±)-**13** with the same enzymes, that is, CALB, lipase PS, and chymotrypsin. Due to unsatisfactory results, we extended our investigation to additional lipases [porcine pancreatic lipase (PPL), lipase from *M. miehei*, lipase

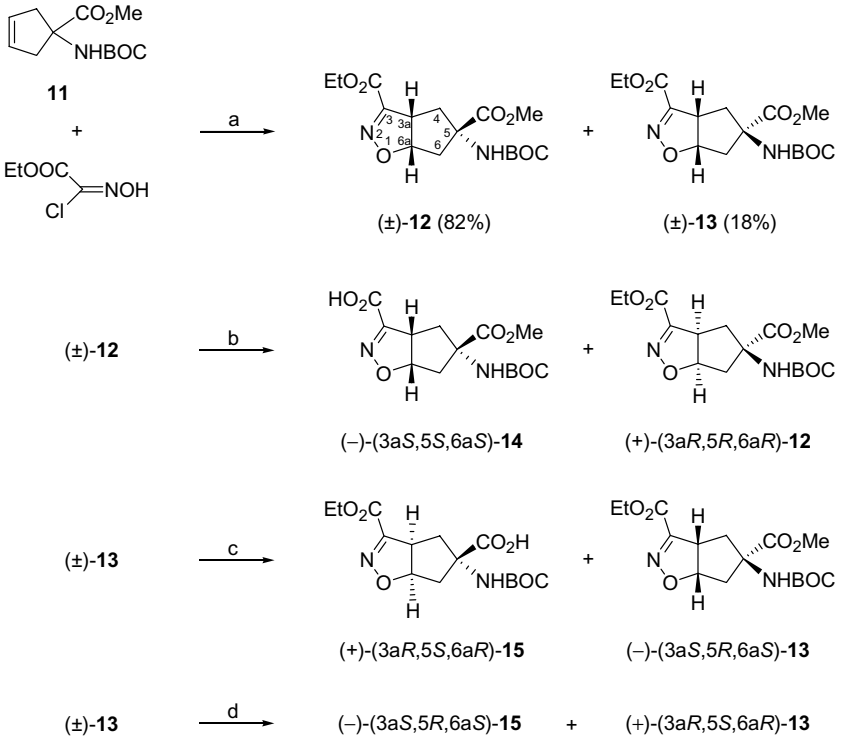

Scheme 1. Reagents and conditions: (a) $NaHCO_3$, AcOEt; (b) CALB, 0.1 M phosphate buffer/acetone; (c) proleather, 0.1 M phosphate buffer/acetone; (d) papain, 0.1 M phosphate buffer/acetone.

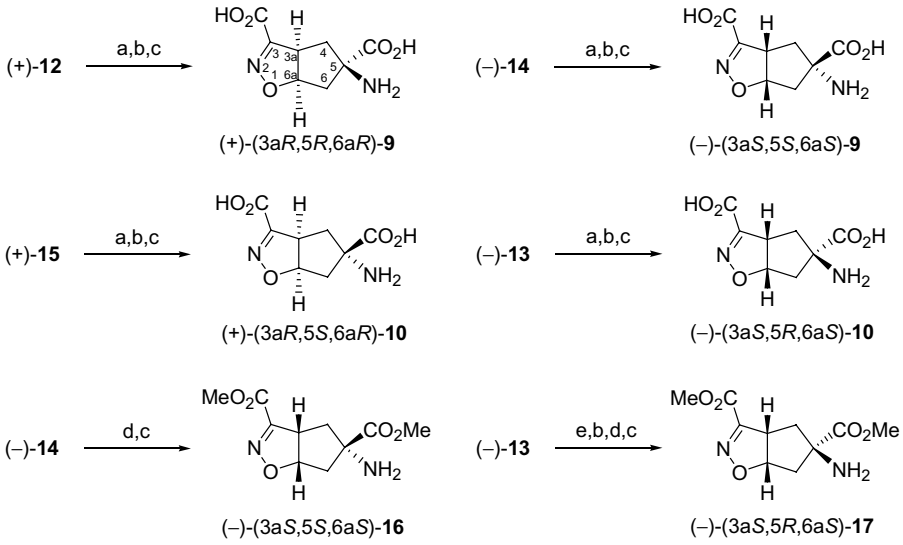

Scheme 2. Reagents and conditions: (a) 1 M NaOH, EtOH; (b) 2 M HCl; (c) 30% CF_3COOH, CH_2Cl_2; (d) CH_2N_2, ether; (e) Na_2CO_3 (aq), EtOH.

from *C. cylindracea* (lipase AY), and lipase AK] and proteases [papain, protease N, and proleather (Subtilysin Carlsberg)]. Within this set of catalysts, only papain and proleather recognized (±)-**13** as a substrate, whereas all the lipases and protease N were totally inactive. Papain- and proleather-catalyzed hydrolyses proceeded with remarkable degrees of enantioselectivity, as evidenced by HPLC analysis of the reaction mixtures (Chiralcel OD-H, see Section 4).

Interestingly, the two proteases, which both regioselectively hydrolyzed the methyl ester linked to position 5, showed a reversed enantiopreference, since papain catalyzed the hydrolysis of diester (−)-**13** to monoacid (−)-**15**, whereas proleather converted enantiomer (+)-**13** into (+)-**15**. For preparative purposes, the kinetic resolution was carried out under the catalysis of proleather, which yielded monoacid (+)-**15** and diester (−)-**13** in ee's higher than 99% at 50% conversion ($E > 500$).[25] Each stereoisomer isolated from the two preparative enzymatic hydrolyses was then transformed into the related final amino acid by standard reactions (Scheme 2).

To assign the absolute configurations to our target compounds, we chose to investigate the experimental and theoretical vibrational circular dichroism spectra and the specific rotation of selected intermediates. Accordingly, levorotatory monoacid (−)-**14** and ethyl methyl ester (−)-**13** were transformed into the corresponding amino dimethyl esters (−)-**16** and (−)-**17** (Scheme 2). The synthesis of (−)-**16** and (−)-**17** was accomplished to avoid the dimers of parent acids that one has to consider, thereby simplifying the pattern of the experimental spectra and shortening the corresponding calculations. Thus, derivative (−)-**14** was sequentially treated with ethereal diazomethane and trifluoroacetic acid to give (−)-**16** in an almost quantitative yield. In analogy, the ethyl ester moiety of (−)-**13** was selectively hydrolyzed and the intermediate monoacid directly transformed into (−)-**17** as reported above.

2.2. Assignment of absolute configurations

2.2.1. Configuration and conformation analysis. 5-Amino-4,5,6,6a-tetrahydro-3a*H*-cyclopenta[*d*]isoxazole-3,5-dicarboxylic acid dimethyl ester contains three stereogenic centers (C-3a, C-5, and C-6a) (Fig. 2A). Owing to the *cis*-relationship existing between the two hydrogens at C-3a and C-6a, which have the same configuration, the number of diastereomers is reduced to four. Two diastereomers, (3a*S*,5*S*,6a*S*)-**16** and (3a*S*,5*R*,6a*S*)-**17**, were chosen for theoretical analyses (Fig. 2A). The remaining two diastereomers (3a*R*,5*R*,6a*R*)-**16** and (3a*R*,5*S*,6a*R*)-**17** are mirror images to the chosen isomers.

The 4,5-dihydroisoxazole moiety of the bicyclic ring is relatively rigid due to the C=N double bond. Conversely, the cyclopentane ring is more flexible than the 4,5-dihydroisoxazole ring. The $-NH_2$ (or $-COOCH_3$) group at C-5 can adopt either an equatorial or axial orientation (Fig. 2B). There is conformational freedom around the two single bonds (C3–C7 and C5–C10) between the bicyclic ring and carboxylate groups. To investigate this conformational mobility, we performed a relaxed potential energy scan (PES), using B3LYP functional and 6-31G* basis set, by varying the dihedral angles, N2–C3–C7–O8 and N9–C5–C10–O11, around these two single bonds. The Newman projections around these two single bonds are shown in Figure 2C. The scan step of the dihedral angle is 20°. For the single bond C3–C7, between the 4,5-dihydroisoxazole ring and the carboxylate group, a 360° PES was performed. For the single bond C5–C10 between the cyclopentane ring and the carboxylate group, a 180° PES was carried out because the environment is almost symmetrical for another 180° dihedral angle change. The results, reported in Figure 3, show the presence of two potential energy minima for each of the two dihedral angles. These minima are at 2° and 182° for the dihedral angle N2–C3–C7–O8 (connecting the 4,5-dihydroisoxazole

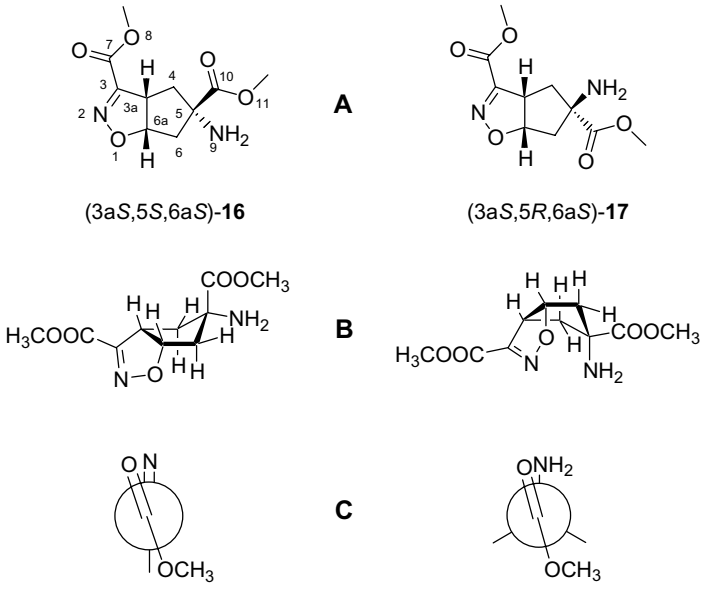

Figure 2. Structures of the investigated diastereomers. (A) (3a*S*,5*S*,6a*S*)-**16** and (3a*S*,5*R*,6a*S*)-**17** epimers. (B) Equatorial and axial orientations at C-5. (C) Newman projections around C3–C7 and C5–C10.

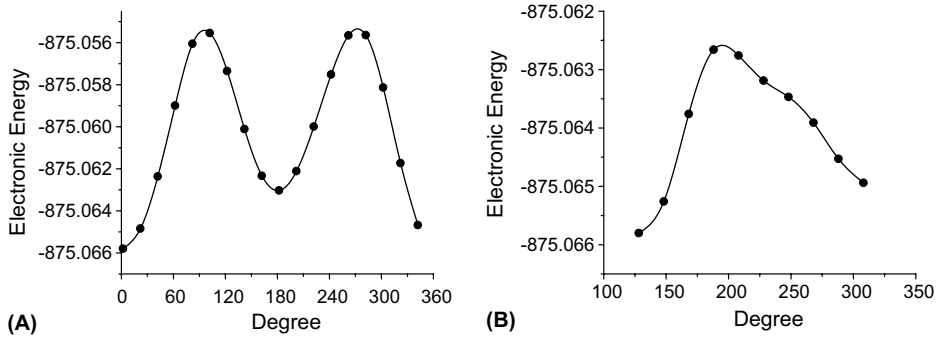

Figure 3. The potential energy scan results for (3a*S*,5*S*,6a*S*)-**16**. (A) Energy (in hartrees) versus dihedral angle N2–C3–C7–O8. (B) Energy (in hartrees) versus dihedral angle N9–C5–C10–O11.

ring to the carboxylate group), and at 128° and 308° for dihedral angle N9–C5–C10–O11 (connecting the cyclopentane ring to the carboxylate group).

These four conformations, in combination with the equatorial and axial orientations at C-5, result in eight possible conformations for each of the two diastereomers studied. Geometry optimization of these eight conformations was undertaken with density functional theory using a B3LYP functional[26,27] and 6-31G* basis set.[28] The most stable five conformations were also investigated using a larger basis set aug-cc-pVDZ[29] for improved accuracy in the calculations. The optimized geometrical parameters for the stable conformations are listed in Table 1. The structure of the lowest energy conformer is displayed in Figure 4 for both the (3a*S*,5*S*,6a*S*)-**16** and (3a*S*,5*R*,6a*S*)-**17** epimers.

2.2.2. Vibrational circular dichroism. The absorbance and vibrational circular dichroism spectra of the five most stable confomers were calculated by using a GAUSSIAN 98 program,[30] at both B3LYP/6-31G* and B3LYP/aug-cc-pVDZ levels. The absorbance and vibrational circular dichroism spectra of (−)-**16** and (−)-**17** were measured in $CDCl_3$ solution.

The comparison of the experimental spectra of amino diester (−)-**16** and the calculated spectra for (3a*S*,5*S*,6a*S*)-**16** (see previous subsection) is shown in Figure 5.

The experimental absorbance spectrum agrees quite well with the calculated absorbance spectrum obtained in the B3LYP/aug-cc-pVDZ calculation, except for one difference. The 1740 cm^{-1} band (labelled as 1) in the experimental spectrum contains two sub-bands, which are not well resolved. However, the B3LYP/aug-cc-pVDZ calculation predicts two well separated corresponding bands. The agreement between the experimental absorbance and the B3LYP/6-31G* predicted spectra is not as good as that found between the experimental

Table 1. Optimized structural parameters[a] for investigated diastereomers (3a*S*,5*S*,6a*S*)-**16** and (3a*S*,5*R*,6a*S*)-**17**

	B3LYP/6-31G*				B3LYP/aug-cc-pVDZ			
Conformer	Energy[b]	*D1*	*D2*	*D3*	Energy[b]	*D1*	*D2*	*D3*
(3a*S*,5*S*,6a*S*)-**16**								
2	−874.862438	0.8	−176.7	150.9(e)	−874.989847	−1.8	−174.6	152.3(e)
1	−874.861389	1.6	4.9	150.3(e)	−874.989984	−1.1	12.5	149.0(e)
6	−874.860838	1.9	−167.4	85.2(a)	−874.988636	−0.4	−165.3	85.7(a)
5	−874.860387	2.8	34.3	78.4(a)	−874.988946	0.5	43.4	79.2(a)
4	−874.859747	178.1	−175.1	154.3(e)	−874.986741	175.6	−172.5	152.6(e)
3	−874.858740	177.7	4.6	150.9(e)	—	—	—	—
8	−874.858164	180.0	−165.3	84.8(a)	—	—	—	—
7	−874.857979	180.0	32.7	78.6(a)	—	—	—	—
(3a*S*,5*S*,6a*S*)-**17**								
6	−874.863450	2.6	180.0	−161.3(e)	−874.991578	0.6	180.0	−160.0(e)
5	−874.862036	2.3	−1.0	−157.8(e)	−874.987907	−0.2	−1.8	−156.7(e)
1	−874.861358	0.1	69.1	−84.1(a)	−874.988963	−3.5	74.6	−85.2(a)
8	−874.861087	180.0	178.3	−161.1(e)	−874.988928	177.9	178.5	−160.0(e)
7	−874.859665	180.0	3.0	−157.7(e)	−874.985415	177.3	34.2	−158.2(e)
2	Not converged	−0.2	−116.8	−88.0(a)	—	—	—	—
3	Not converged	180.0	72.6	−83.2(a)	—	—	—	—
4	Not converged	171.5	−119.1	−88.0(a)	—	—	—	—

[a] Dihedral angles D_1, D_2 and D_3 represent, respectively, the angles of N2–C3–C7–O8, N9–C5–C10–O11 and C6a–C6–C5–C10 (a and e indicate, respectively, the axial and equatorial orientation of the carboxylic group on the cyclopentane ring).
[b] Gibbs energy (in units of hartree).

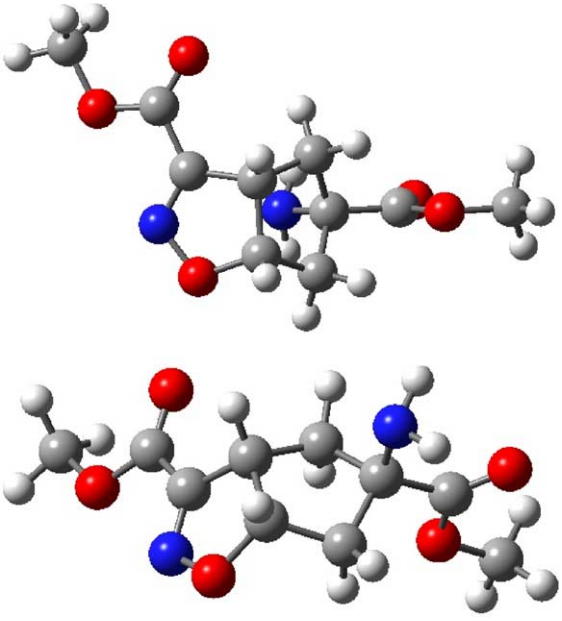

Figure 4. B3LYP/6-31G* optimized structures for the lowest energy conformer of (3a*S*,5*S*,6a*S*)-**16** (top) and of (3a*S*,5*R*,6a*S*)-**17** (bottom).

absorbance and the B3LYP/aug-cc-pVDZ predicted spectra. In the experimental absorbance spectrum, the region from 1700–1400 cm^{-1} shows two bands (labelled as 2 and 3), while the B3LYP/-631G* predicted spectrum shows two separated bands, each for the corresponding experimental bands 2 and 3. The experimental VCD spectrum agrees quite well with the calculated VCD spectrum obtained in both the B3LYP/6-31G* and the B3LYP/aug-cc-pVDZ calculations, except for one significant difference; that is, the negative–positive couplet in the 1300–1250 cm^{-1} region (labelled as 6 and 7) is clearly seen in the experimental spectrum, whereas the corresponding bands in the predicted VCD spectra are characterized by low relative intensities. The major negative–positive couplet in the 1250–1200 cm^{-1} region (labelled as 8 and 9) observed in the experimental VCD spectrum, however is reproduced in the predicted spectra.

The experimental spectra for amino diester (−)-**17** and the calculated spectra for (3a*S*,5*R*,6a*S*)-**17** (see previous subsection) are shown in Figure 6.

The experimental absorbance spectrum agrees quite well with the calculated absorbance spectrum obtained in both the B3LYP/6-31G* and the B3LYP/aug-cc-pVDZ calculations, except for the following significant differences. The experimental bands at 1740 and 1230 cm^{-1} (labelled as 1 and 7, respectively) do not show any splittings, at variance with the predicted spectra, in which well separated splittings for the corresponding bands are observed. In the VCD spectra, a good agreement is observed for the negative–positive couplet ~1300 cm^{-1} (labelled 5 and 6) in both the experimental and predicted spectra. Conversely, the experimental intensity of the positive–negative couplet (labelled 7) at ~1220 cm^{-1} is smaller than that in the predicted spectra. The reason for such a discrepancy is that this experimental band is accompanied by two not well resolved sub-bands. These two bands have oppositely signed VCDs, which tend to cancel each other when they are not well separated. In the predicted spectra, the corresponding two bands are well separated from each other, so the intensity is larger. Finally, the positive VCD band at 1050 cm^{-1} (labelled as 12) and negative band at 950 cm^{-1} (labelled as 13) are clearly evident in both experimental and predicted spectra.

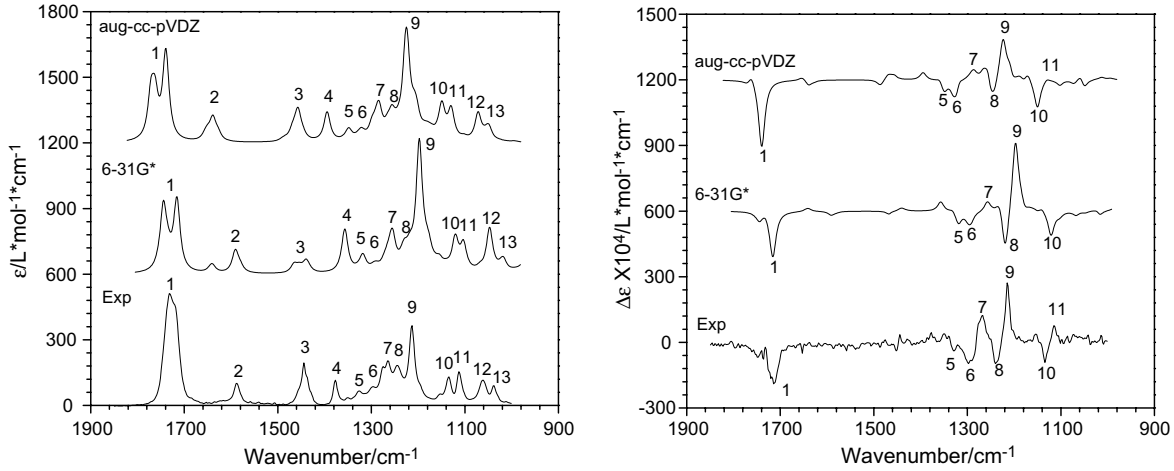

Figure 5. The comparison between the experimental spectra of (−)-**16** and the predicted spectra for (3a*S*,5*S*,6a*S*)-**16** isomer. Left: IR absorbance spectra. Right: VCD spectra.

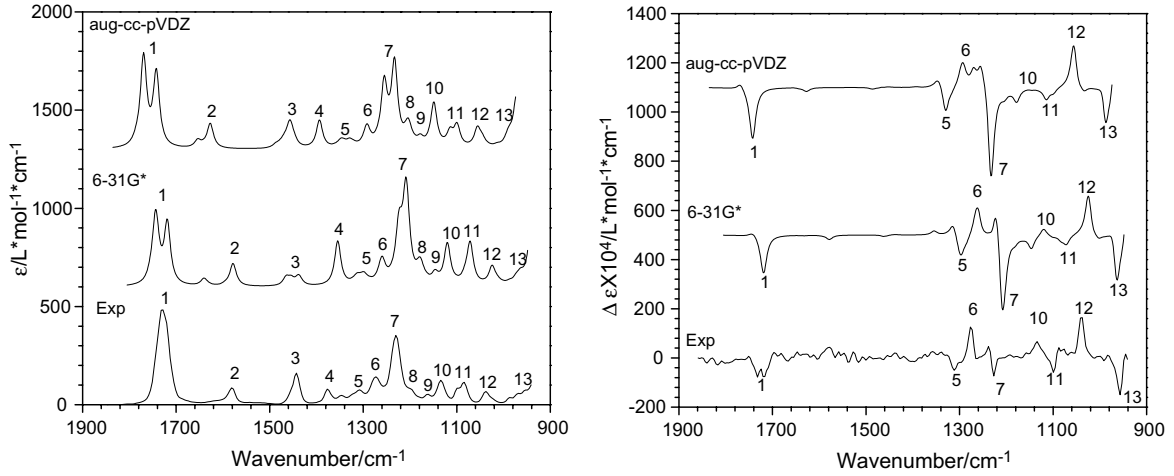

Figure 6. The comparison between the experimental spectra of (−)-**17** and the predicted spectra for (3a*S*,5*R*,6a*S*)-**17** isomer. Left: IR absorbance spectra. Right: VCD spectra.

Based on the comparison of experimental VCD spectra with those predicted for the two epimers, it can be concluded that the absolute configuration for compound (−)-**16** is (3a*S*,5*S*,6a*S*) and that for compound (−)-**17** is (3a*S*,5*R*,6a*S*). As a consequence, the absolute configuration can be assigned to the related epimeric amino acids [(−)-(3a*S*,5*S*,6a*S*)-**9** and (−)-(3a*S*,5*R*,6a*S*)-**10**] and to their enantiomers [(+)-(3a*R*,5*R*,6a*R*)-**9** and (+)-(3a*R*,5*S*,6a*R*)-**10**, respectively].

2.2.3. Optical rotation. The optical rotations of the two epimeric bicyclic isoxazolines were measured at the sodium D line. To eliminate the influence of solute–solute interactions, intrinsic rotation[31] (specific rotation in the limit of zero concentration) was obtained. The experimental specific rotation against concentration is shown for both compounds in Figure 7 and was analyzed with the weighted least squares method. The intrinsic rotation values are -123.0 ± 1.3 for (−)-**16** and -167.0 ± 1.3 for (−)-**17** (in units of degree $\times$ $g^{-1} \times mL \times dm^{-1}$).

The specific rotations of the stable conformers of the two diastereomers were calculated at both the B3LYP/6-31G* and B3LYP/aug-cc-pVDZ level. The predicted specific rotations for the diastereomers are the population-weighted sum of the specific rotations of individual conformers. The calculated specific rotations are summarized in Tables 2 and 3.

The calculated specific rotations for (3a*S*,5*S*,6a*S*)-**16** are −206.7 in the B3LYP/6-31G* calculation and −210.7 in the B3LYP/aug-cc-pVDZ calculation (Table 2). The calculated specific rotations for (3a*S*,5*R*,6a*S*)-**17** are −277.3 in the B3LYP/6-31G* calculation and −295.2 in the B3LYP/aug-cc-pVDZ calculation (Table 3). Since the intrinsic rotations observed for (−)-**16** and (−)-**17** are −123 and −167, respectively, the magnitudes of the calculated specific rotations are larger than the experimental intrinsic rotations by ~1.7. Nevertheless, based on the relative magnitude of intrinsic rotations, the configuration of the amino diester with the smaller absolute experimental intrinsic rotation is assigned as

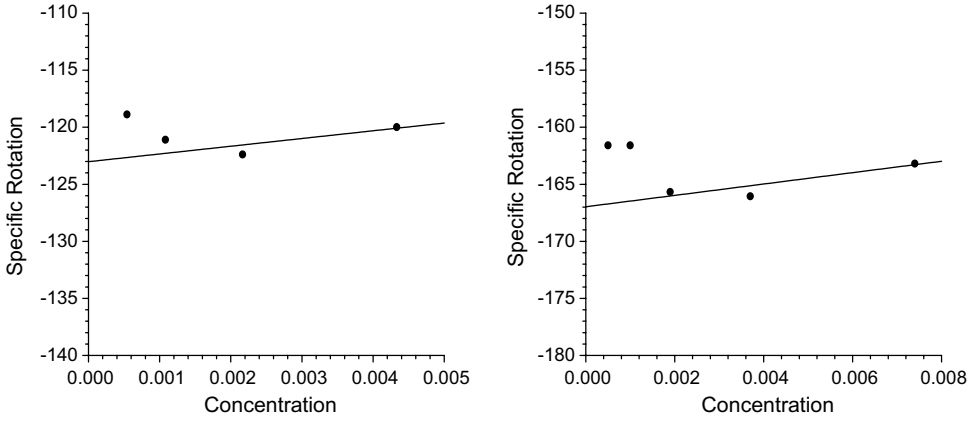

Figure 7. The experimental specific rotation versus concentration (g/mL) for the two epimers under study. Left: compound (−)-**16**, the data were fit to $[\alpha]_D = +677.5*c - 123.0$. Right: compound (−)-**17**, the data were fit to $[\alpha]_D = +498.4*c - 167.0$.

Table 2. The calculated specific rotation of (3a*S*,5*S*,6a*S*)-**16** diastereomer and the observed intrinsic rotation of derivative (−)-**16**

Conformer	Population	$[\alpha]_D$
B3LYP/6-31G*		
2	0.5935	−206.6
1	0.1955	−197.7
6	0.1090	−219.6
5	0.0676	−222.8
4	0.0344	−187.9
Population weighted specific rotation		−206.7
Observed intrinsic rotation		−123.0
B3LYP/aug-cc-pVDZ		
1	0.4049	−190.2
2	0.3502	−200.4
5	0.1348	−268.4
6	0.0971	−259.2
4	0.0130	−169.4
Population weighted specific rotation		−210.7
Observed intrinsic rotation		−123.0

Table 3. The calculated specific rotation of (3a*S*,5*S*,6a*S*)-**17** diastereomer and the observed intrinsic rotation of derivative (−)-**17**

Conformer	Population	$[\alpha]_D$
B3LYP/6-31G*		
6	0.6980	−277.5
5	0.1561	−262.6
1	0.0761	−312.9
8	0.0571	−267.1
7	0.0127	−275.5
Population weighted specific rotation		−277.3
Observed intrinsic rotation		−167.0
B3LYP/aug-cc-pVDZ		
6	0.8733	−297.5
1	0.0547	−351.8
8	0.0527	−267.7
5	0.0179	−276.7
7	0.0014	−388.6
Population weighted specific rotation		−295.2
Observed intrinsic rotation		−167.0

that of the stereoisomer predicted to have a smaller specific rotation. Thus, the absolute configuration of (−)-**16** is assigned as (3a*S*,5*S*,6a*S*) and that of (−)-**17** as (3a*S*,5-*R*,6a*S*). These assignments are consistent with those deduced from VCD spectra.

3. Conclusion

The use of highly selective enzyme-catalyzed hydrolyses allowed the synthesis of both enantiomeric pairs of two bicyclic amino acids, whose racemates had previously been prepared and tested at ionotropic as well as metabotropic glutamate receptors. The absolute configuration was attributed to the compounds under investigation by comparing the experimental VCD features of two key intermediates with those obtained from theoretical calculations. A parallel experimental/theoretical protocol applied to the values the specific rotation led to the same configurational assignment obtained through VCD. The biopharmacological screening of the target enantiopure stereoisomers is currently underway and will be reported in due course.

4. Experimental

4.1. General

Lipase B from *C. antarctica* (CALB) was bought from Roche Diagnostics (CHIRAZYME L-2). Chymotrypsin, papain, porcine pancreatic lipase (PPL), lipases from *M. miehei* and from *P. cepacia* (lipase PS) were purchased from Fluka. Protease N, proleather (Subtilysin Carlsberg), lipase AK and lipase from *C. cylindracea* (lipase AY) were obtained from Amano Pharmaceuticals Co.

Ethyl 2-chloro-2-(hydroxyimino)acetate[32] and methyl *N*-(*tert*-butoxycarbonyl)-1-amino-cyclopent-3-enecarb-

oxylate **11**[24] were prepared according to literature procedures. ^{1}H NMR and ^{13}C NMR spectra were recorded with a Varian Mercury 300 (300 MHz) spectrometer in $CDCl_3$, CD_3OD, and D_2O solution at 20 °C. Chemical shifts (δ) are expressed in ppm and coupling constants (J) in hertz. HPLC analyses were performed with a Jasco PU-980 pump equipped with a UV–vis detector Jasco UV-975 and with a Sedex 750 light scattering detector. Rotary power determinations were carried out with either a Autopol IV polarimeter [for (−)-**16** and (−)-**17**)] or a Perkin–Elmer 241 polarimeter coupled with a Haake N3-B thermostat (for the remaining compounds). TLC analyses were performed on commercial silica gel 60 F_{254} aluminum sheets; spots were further evidenced by spraying with a dilute alkaline potassium permanganate solution or with ninhydrin. Melting points were determined on a model B 540 Büchi apparatus and are uncorrected.

The infrared and VCD spectra were measured and analyzed as described previously.[33] The spectra were recorded on a commercial Fourier transform VCD spectrometer, Chiralir. The VCD spectra were recorded with three hour data collection time at 4 cm^{-1} resolution. Spectra were measured in $CDCl_3$ solutions at a concentration of about 15 mg/mL. The sample was held in a variable path length cell with BaF_2 windows. In the absorption spectra presented, the solvent absorption was subtracted out. In the VCD spectra presented, the raw VCD spectrum of the solvent was subtracted. Intrinsic rotation, $\{\alpha\}_D$ (specific rotation in the limit of zero concentration), was extracted as described previously,[31] from a plot of experimental specific rotation, $[\alpha]_D$, versus concentration. The specific rotations were measured at 589 nm in $CHCl_3$ solutions, using a Autopol IV polarimeter.

The vibrational frequencies, absorption and VCD intensities were calculated for the two diastereomers using GAUSSIAN 98 program.[30] The calculations used the density functional theory with B3LYP functional[26,27] and 6-31G* and aug-cc-pVDZ basis sets.[28] The procedure for calculating the VCD intensities using DFT theory is due to Cheeseman et al.[29] as implemented in the GAUSSIAN 98 program. The theoretical absorption and VCD spectra of the two diastereomers were simulated with Lorentzian band shapes and 8 cm^{-1} half-width. The B3LYP/6-31G* calculated frequencies were scaled with 0.96. The specific rotations were calculated using the Dalton program.[34]

4.2. Synthesis of (±)-(3a*R**,5*R**,6a*R**)-5-*tert*-Butoxycarbonylamino-4,5,6,6a-tetrahydro-3a*H*-cyclopenta[*d*]-isoxazole-3,5-dicarboxylic acid 3-ethyl ester, 5-methyl ester and (±)-(3a*R**,5*S**,6a*R**)-5-*tert*-butoxycarbonylamino-4,5,6,6a-tetrahydro-3a*H*-cyclopenta[*d*]isoxazole-3,5-dicarboxylic acid 3-ethyl ester, 5-methyl ester, (±)-12 and (±)-13

To a solution of **11** (3.0 g, 12.44 mmol) in AcOEt (70 mL) was added ethyl 2-chloro-2-(hydroxyimino)acetate (3.77 g, 24.88 mmol) and $NaHCO_3$ (8.0 g). The mixture was vigorously stirred for three days and the progress of the reaction monitored by TLC (petroleum ether/AcOEt, 7:3). Water was added to the reaction mixture and the organic layer separated and dried over anhydrous Na_2SO_4. The crude material, obtained after evaporation of the solvent, was submitted to a silica gel column chromatography (petroleum ether/AcOEt, 4:1) to give 3.06 g of (±)-**12** and 0.671 g of (±)-**13**. Overall yield: 84%.

4.2.1. (±)-(3a*R,5*R**,6a*R**)-5-*tert*-Butoxycarbonylamino-4,5,6,6a-tetrahydro-3a*H*-cyclopenta[*d*]isoxazole-3,5-dicarboxylic acid 3-ethyl ester, 5-methyl ester (±)-12.** Colorless needles from isopropyl ether, mp 138–139 °C. R_f 0.22 (cyclohexane/AcOEt, 7:3). HPLC retention time: 20.18 min (column: LiChrospher Si 60 Merck; eluant: petroleum ether/AcOEt, 4:1; flow rate: 1 mL/min; λ = 254 nm); (+)-**12**: 16.77 min; (−)-**12**: 12.29 min (column: CHIRALCEL OD-H, Diacel; eluant: petroleum ether/2-propanol 85:15 + 0.4% formic acid; flow rate: 0.5 mL/min; λ = 254 nm). ^{1}H NMR ($CDCl_3$): 1.34 (t, J = 6.9, 3H), 1.38 (s, 9H), 2.41 (m, 2H), 2.63 (dd, J = 9.4, 14.7, 1H), 2.80 (br d, J = 13.8, 1H), 3.72 (s, 3H), 4.02 (ddd, J = 2.4, 9.4, 9.4, 1H), 4.32 (m, 2H), 4.95 (br s, 1H), 5.33 (ddd, J = 3.2, 7.5, 9.4, 1H). ^{13}C NMR ($CDCl_3$): 14.50, 28.47, 39.38, 45.60, 50.93, 53.11, 62.34, 65.75, 80.48, 88.83, 154.40, 154.96, 160.34, 173.14. FT-IR (film, cm^{-1}): 3370, 2980, 1719, 1587, 1508, 1368, 1276, 1212, 1164, 1070, 934. Anal. Calcd for ($C_{16}H_{24}N_2O_7$) (356.37): C, 53.92; H, 6.79; N, 7.86. Found C, 53.77; H, 6.88; N, 7.98.

4.2.2. (±)-(3a*R,5*S**,6a*R**)-5-*tert*-Butoxycarbonylamino-4,5,6,6a-tetrahydro-3a*H*-cyclopenta[*d*]isoxazole-3,5-dicarboxylic acid 3-ethyl ester, 5-methyl ester (±)-13.** Colorless needles from isopropyl ether, mp 118–119 °C. R_f 0.25 (cyclohexane/AcOEt, 7:3). HPLC retention time: 18.42 min (column: LiChrospher Si 60 Merck; eluant: petroleum ether/AcOEt 4:1; flow rate: 1 mL/min; λ = 254 nm); (+)-**13**: 22.76 min; (−)-**13**: 20.80 min (column: CHIRALCEL OD-H, Diacel; eluant: petroleum ether/2-propanol 95:5 + 0.1% acetic acid; flow rate: 0.5 mL/min; λ = 254 nm). ^{1}H NMR ($CDCl_3$): 1.36 (t, J = 7.2, 3H), 1.42 (s, 9H), 2.44 (dd, J = 5.1, 14.1, 1H), 2.55 (m, 2H), 2.67 (dd, J = 6.6, 13.8, 1H), 3.71 (s, 3H), 4.05 (m, 1H), 4.34 (q, J = 7.2, 2H), 5.10 (br s, 1H), 5.37 (ddd, J = 5.1, 6.6, 10.2, 1H). ^{13}C NMR ($CDCl_3$): 14.43, 28.52, 40.39, 45.80, 51.13, 53.22, 62.35, 66.15, 80.68, 88.95, 154.20, 155.06, 160.38, 172.14. FT-IR (film, cm^{-1}): 3369, 2923, 1719, 1583, 1512, 1459, 1368, 1279, 1229, 1165, 1089, 1020, 928. Anal. Calcd for $C_{16}H_{24}N_2O_7$ (356.37): C, 53.92; H, 6.79; N, 7.86. Found C, 53.80; H, 6.89; N, 7.93.

4.3. Preparative enzymatic hydrolysis of diester (±)-12

To a suspension of (±)-**12** (1.0 g, 2.80 mmol) in 0.1 M phosphate buffer pH 8.0 (80 mL) and acetone (20 mL), CALB (1.0 g) was added and the mixture gently stirred at rt for five days. The progress of the reaction was monitored by HPLC (column: CHIRALCEL OD-H, Diacel; eluant: petroleum ether/2-propanol 85:15 + 0.4% formic acid; flow rate: 0.5 mL/min; λ = 254 nm). The reaction spontaneously stopped at 50% conversion to yield

monoacid (−)-**14** and residual ester (+)-**12** in an ee higher than 99%. Solid $NaHCO_3$ was added, then the reaction mixture extracted with diethyl ether and the pooled organic layers were evaporated to recover the residual ester (+)-**12** (450 mg). The aqueous phase was made acidic with HCl (2 M) with monoacid (−)-**14** (400 mg) was obtained after extraction with diethyl ether, drying over anhydrous Na_2SO_4 and evaporation of the solvent.

(+)-(3a*R*,5*R*,6a*R*)-**12**: $[\alpha]_D^{20} = +93.0$ (*c* 1.0, $CHCl_3$).

4.3.1. (−)-(3a*S*,5*S*,6a*S*)-5-*tert*-Butoxycarbonylamino-4,5,6,6a-tetrahydro-3a*H*-cyclopenta[*d*]isoxazole-3,5-dicarboxylic acid 5-methyl ester (−)-14. $[\alpha]_D^{20} - 90.0$ (*c* 1.0, $CHCl_3$). Colorless needles from methanol, mp 113–116 °C. R_f 0.32 (chloroform/methanol 95:5 + 50 μL acetic acid). HPLC retention time: 18.98 min (column: CHIRALCEL OD-H, Diacel; eluant: petroleum ether/2-propanol 85:15 + 0.4% formic acid; flow rate: 0.5 mL/min; $\lambda = 254$ nm). ^{1}H NMR (CD_3OD): 1.39 (s, 9H), 2.49 (m, 3H), 2.77 (br d, $J = 14.1$, 1H), 3.69 (s, 3H), 4.03 (m, 1H), 5.35 (m, 1H). ^{13}C NMR (CD_3OD): 27.60, 38.88, 44.44, 50.80, 52.02, 65.55, 79.43, 89.01, 154.66, 156.30, 161.81, 173.90. FT-IR (film, cm^{-1}): 3382, 2978, 1711, 1588, 1509, 1434, 1394, 1368, 1254, 1214, 1163, 1071, 935, 752. Anal. Calcd for $C_{14}H_{20}N_2O_7$ (328.32): C, 51.22; H, 6.14; N, 8.53. Found C, 51.46; H, 6.32; N, 8.34.

4.4. Preparative enzymatic hydrolysis of diester (±)-13

To a suspension of (±)-**13** (700 mg, 1.96 mmol) in 0.1 M phosphate buffer pH 8.0 (40 mL) and acetone (10 mL), proleather (1.0 g) was added and the mixture gently stirred at rt for three days. The progress of the reaction was monitored by HPLC (column: CHIRALCEL OD-H, Diacel; eluant: petroleum ether/2-propanol 95:5 + 0.1% acetic acid; flow rate: 0.5 mL/min; $\lambda = 254$ nm). When the enzymatic hydrolysis reached 50% conversion, solid $NaHCO_3$ was added. The reaction mixture was extracted with diethyl ether and the pooled organic layers evaporated to recover the residual ester (−)-**13** (270 mg). The aqueous phase was made acidic with HCl (2 M) with monoacid (+)-**15** (250 mg) being obtained after extraction with diethyl ether, drying over anhydrous Na_2SO_4 and evaporation of the solvent.

(−)-(3a*S*,5*R*,6a*S*)-**13**: $[\alpha]_D^{20} = -38.7$ (*c* 2.10, $CHCl_3$).

4.4.1. (+)-(3a*R*,5*S*,6a*R*)-5-*tert*-Butoxycarbonylamino-4,5,6,6a-tetrahydro-3a*H*-cyclopenta[*d*]isoxazole-3,5-dicarboxylic acid 3-ethyl ester (+)-15. $[\alpha]_D^{20} = +81.9$ (*c* 0.80, $CHCl_3$). Colorless oil. R_f 0.25 (chloroform/methanol 95:5 + 50 μL acetic acid). HPLC retention time: 26.13 min (column: CHIRALCEL OD-H, Diacel; eluant: petroleum ether/2-propanol 95:5 + 0.1% acetic acid; flow rate: 0.5 mL/min; $\lambda = 254$ nm). ^{1}H NMR ($CDCl_3$): 1.37 (t, $J = 7.2$, 3H), 1.43 (s, 9H), 2.47 (m, 1H), 2.56 (br d, $J = 7.8$, 2H), 2.68 (m, 1H), 4.08 (m, 1H), 4.35 (q, $J = 7.2$, 2H), 5.38 (ddd, $J = 6.0$, 6.9, 10.5, 1H). ^{13}C NMR ($CDCl_3$): 14.52, 26.83, 28.57, 30.07, 41.26, 45.01, 51.05, 62.50, 66.08, 88.81, 154.09, 160.57, 176.67. FT-IR (film, cm^{-1}): 3360, 2980, 1716, 1583, 1513, 1369, 1232, 1163, 1021, 932, 754. Anal. Calcd for $C_{15}H_{22}N_2O_7$ (342.34): C, 52.63; H, 6.48; N. 8.18. Found C, 52.54; H, 6.55; N, 8.31.

4.5. Synthesis of (−)-(3a*S*,5*S*,6a*S*)-5-amino-4,5,6,6a-tetrahydro-3a*H*-cyclopenta[*d*]isoxazole-3,5-dicarboxylic acid dimethyl ester (−)-16

Monoacid (−)-**14** (200 mg, 0.61 mmol) was treated with ethereal diazomethane (2 mL). Diethyl ether was then removed under vacuum and the residue reacted with a 30% dichloromethane solution of trifluoroacetic acid (2 mL) at 0 °C. The solution was stirred at rt until disappearance of the starting material (3 h). The volatiles were removed under vacuum and the residue treated with a 20% $NaHCO_3$ solution (8 mL) and extracted with AcOEt (3 × 5 mL). The pooled organic extracts were dried over anhydrous Na_2SO_4 and concentrated under vacuum to obtain (−)-**16** (60 mg) in 40% overall yield.

4.5.1. (−)-(3a*S*,5*S*,6a*S*)-5-Amino-4,5,6,6a-tetrahydro-3a*H*-cyclopenta[*d*]isoxazole-3,5-dicarboxylic acid dimethyl ester (−)-16. Colorless oil. $[\alpha]_D^{20} = -120.0$ (*c* 0.43, $CHCl_3$). R_f 0.40 (cyclohexane/AcOEt, 3:7); ^{1}H NMR ($CDCl_3$): 1.64 (br s, 2H), 2.18 (d, $J = 14.7$, 2H), 2.38 (dd, $J = 9.3$, 14.4, 1H), 2.53 (dd, $J = 6.6$, 15.0, 1H), 3.73 (s, 3H), 3.88 (s, 3H), 4.00 (m, 1H), 5.37 (m, 1H). ^{13}C NMR ($CDCl_3$): 43.06, 47.03, 51.69, 53.01, 53.04, 64.98, 89.32, 153.98, 161.45, 176.44. FT-IR ($CDCl_3$ solution, cm^{-1}): 1731, 1588, 1444, 1377, 1326, 1300, 1264, 1245, 1214, 1135, 1112, 1062, 1039. Anal. Calcd for $C_{10}H_{14}N_2O_5$ (242.23): C, 49.58; H, 5.83: N, 11.56. Found C, 49.38; H, 5.97; N, 11.78.

4.6. Synthesis of (−)-(3a*S*,5*R*,6a*S*)-5-amino-4,5,6,6a-tetrahydro-3a*H*-cyclopenta[*d*]isoxazole-3,5-dicarboxylic acid dimethyl ester (−)-17

Diester (−)-**13** (300 mg, 0.84 mmol) was dissolved in ethanol (10 mL) and potassium carbonate then added (290 mg, 2.1 mmol). The mixture was stirred at rt for 4 h and the progress of the reaction monitored by TLC (chloroform/methanol 95:5 + 50 μL acetic acid). After filtration and evaporation of the solvent, the residue was dissolved in HCl (2 M) and extracted with ethyl acetate. The organic layers were dried and evaporated, and the crude residue treated with ethereal diazomethane and subsequently with trifluoroacetic acid as described above. The volatiles were removed under vacuum and the residue treated with a 20% $NaHCO_3$ solution (8 mL) and extracted with AcOEt (3 × 5 mL). The pooled organic extracts were dried over anhydrous Na_2SO_4 and concentrated under vacuum to obtain (−)-**17** (70 mg) in 35% overall yield.

4.6.1. (−)-(3a*S*,5*R*,6a*S*)-5-Amino-4,5,6,6a-tetrahydro-3a*H*-cyclopenta[*d*]isoxazole-3,5-dicarboxylic acid dimethyl ester (−)-17. $[\alpha]_D^{20} - 166.1$ (*c* 0.37, $CHCl_3$). R_f 0.15 (cyclohexane/AcOEt 3:7); ^{1}H NMR ($CDCl_3$): 1.55 (br s, 2H), 2.20 (m, 1H), 2.32 (m, 2H), 2.50 (m, 1H), 3.71 (s, 3H), 3.84 (s, 3H), 4.15 (m, 1H), 5.47 (m, 1H). ^{13}C NMR ($CDCl_3$): 42.94, 46.57, 51.08, 53.12, 53.86,

62.02, 90.19, 153.93, 167.31, 176.81. FT-IR ($CDCl_3$ solution, cm^{-1}): 1730, 1581, 1444, 1376, 1308, 1273, 1229, 1162, 1134, 1090, 1038. Anal. Calcd for $C_{10}H_{14}N_2O_5$ (242.23): C, 49.58; H, 5.83; N, 11.56. Found C, 49.45; H, 5.99; N, 11.67.

4.7. Synthesis of 5-amino-4,5,6,6a-tetrahydro-3a*H*-cyclopenta[*d*]isoxazole-3,5-dicarboxylic acids (+)-9 and (−)-9

Diester (+)-**12** (200 mg, 0.56 mmol) was dissolved in EtOH and treated with 1 M NaOH (2.0 mL) at rt overnight. The solution was made acidic with 2 M HCl and then repeatedly extracted with AcOEt. The pooled organic extracts were dried over anhydrous Na_2SO_4, the solvent evaporated off and the residue treated with a 30% dichloromethane solution of trifluoroacetic acid (1.5 mL) at 0 °C. After stirring at rt for 3 h, the volatiles were removed under vacuum, and the residue, crystallized from water/methanol, filtered and washed sequentially with methanol and ethyl ether and dried in vacuo at 50 °C to give amino acid (+)-**9** (90 mg, 74% overall yield) as white prisms.

4.7.1. (+)-(3a*R*,5*R*,6a*R*)-5-Amino-4,5,6,6a-tetrahydro-3a*H*-cyclopenta[*d*]isoxazole-3,5-dicarboxylic acid (+)-9.

$[\alpha]_D^{20} = +199.0$ (*c* 0.10, H_2O). Decomposes in the range 173–180 °C. HPLC retention time: 12.79 min (column: CHIROBIOTIC TAG, Astec; eluant: [ethanol/methanol, 3:2]/water 4:1 + 50 mM ammonium acetate + 0.1% acetic acid; flow rate: 1 mL/min; light scattering detection). FT-IR (KBr disk, cm^{-1}): 3408, 3243, 2515, 1907, 1677, 1625, 1381. Anal. Calcd for $C_8H_{10}N_2O_5 \times 1H_2O$ (232.19): C, 41.38; H, 5.21; N, 12.06. Found C, 41.25; H, 5.28; N, 12.19. The ^1H NMR and ^{13}C NMR spectra of (+)-**9** were identical to those previously reported for the racemate.[20]

Treatment of monoacid (−)-**14** (200 mg, 0.61 mmol) along with the same procedure described for diester (+)-**12** afforded amino acid (−)-**9** (80 mg, 60% overall yield) as white prisms.

4.7.2. (−)-(3a*S*,5*S*,6a*S*)-5-Amino-4,5,6,6a-tetrahydro-3a*H*-cyclopenta[*d*]isoxazole-3,5-dicarboxylic acid (−)-9.

$[\alpha]_D^{20} - 202.0$ (*c* 0.11, H_2O). Decomposes in the range 173–180 °C. HPLC retention time: 22.10 min (column: CHIROBIOTIC TAG, Astec; eluant: [ethanol/methanol, 3:2]/water 4:1 + 50 mM ammonium acetate + 0.1% acetic acid; flow rate: 1 mL/min; light scattering detection). FT-IR (KBr disk, cm^{-1}): 3408, 3243, 2515, 1907, 1677, 1625, 1381. Anal. Calcd for $C_8H_{10}N_2O_5 \times 1H_2O$ (232.19): C, 41.38; H, 5.21; N, 12.06. Found C, 41.56; H, 5.09; N, 12.25. The ^1H NMR and ^{13}C NMR spectra of (−)-**9** were identical to those previously reported for the racemate.[20]

4.8. Synthesis of 5-amino-4,5,6,6a-tetrahydro-3a*H*-cyclopenta[*d*]isoxazole-3,5-dicarboxylic acids (−)-10 and (+)-10

Diester (−)-**13** (200 mg, 0.56 mmol) was dissolved in EtOH and treated with 1 M NaOH (2.0 mL) at rt overnight. The solution was made acidic with 2 M HCl and then repeatedly extracted with AcOEt. Treatment of the crude diacid along with the experimental protocol reported for (+)-**9** provided amino acid (−)-**10** (85 mg, 64% overall yield) as white prisms.

4.8.1. (−)-(3a*S*,5*R*,6a*S*)-5-Amino-4,5,6,6a-tetrahydro-3a*H*-cyclopenta[*d*]isoxazole-3,5-dicarboxylic acid (−)-10.

$[\alpha]_D^{20} = -128.0$ (*c* 0.10, H_2O). Decomposes in the range 200–210 °C. HPLC retention time: 13.63 min (column: CHIROBIOTIC TAG, Astec; eluant: [ethanol/methanol, 3:2]/water 4:1 + 50 mM ammonium acetate + 0.1% acetic acid; flow rate: 1 mL/min; light scattering detection). FT-IR (KBr disk, cm^{-1}): 3430, 3262, 1722, 1625, 1574, 1383. Anal. Calcd for $C_8H_{10}N_2O_5 \times 1H_2O$ (232.19): C, 41.38; H, 5.21; N, 12.06. Found C, 41.47; H, 5.16; N, 11.95. The ^1H NMR and ^{13}C NMR spectra of (−)-**10** matched those reported for the racemate.[20]

Treatment of monoacid (+)-**15** (200 mg, 0.58 mmol) following the procedure described for diester (+)-**12** produced 95 mg (78% overall yield) of amino acid (+)-**10** as white prisms.

4.8.2. (+)-(3a*R*,5*S*,6a*R*)-5-Amino-4,5,6,6a-tetrahydro-3a*H*-cyclopenta[*d*]isoxazole-3,5-dicarboxylic acid (+)-10.

$[\alpha]_D^{20} = +129.0$ (*c* 0.10, H_2O). Decomposes in the range 200–210 °C. HPLC retention time: 9.87 min (column: CHIROBIOTIC TAG, Astec; eluant: [ethanol/methanol, 3:2]/water 4:1 + 50 mM ammonium acetate + 0.1% acetic acid; flow rate: 1 mL/min; light scattering detection). FT-IR (KBr disk, cm^{-1}): 3430, 3262, 1722, 1625, 1574, 1383. Anal. Calcd for $C_8H_{10}N_2O_5 \times 1H_2O$ (232.19): C, 41.38; H, 5.21; N, 12.06. Found C, 41.19; H, 5.41; N, 12.28. The ^1H NMR and ^{13}C NMR spectra of (+)-**10** matched those reported for the racemate.[20]

Acknowledgements

This work was financially supported by MIUR (COFIN 2001) Rome, Università degli Studi di Milano, and the National Science Foundation. The authors thank Dr. K. Ruud for providing a developmental version of the DALTON program, which was used for calculating the specific rotations reported here. Any opinions, findings, and conclusions or recommendations expressed in this material are those of the author(s) and do not necessarily reflect the views of the National Science Foundation.

References

1. *Excitatory Amino Acids and Synaptic Transmissions*; Wheal, H. V., Thomson, A. M., Eds.; Academic: London, 1995.
2. Bräuner-Osborne, H.; Egebjerg, J.; Nielsen, E. Ø.; Madsen, U.; Krogsgaard-Larsen, P. *J. Med. Chem.* **2000**, *43*, 2609–2645.
3. Ozawa, S.; Kamiya, H.; Tsuzuki, K. *Prog. Neurobiol.* **1998**, *54*, 581–618.

4. *The Ionotropic Glutamate Receptors*; Monaghan, D. T., Wenthold, R. J., Eds.; Humana: Totowa, NJ, 1997.
5. *Handbook of Experimental Pharmacology, Ionotropic Glutamate Receptors in the CNS*; Jonas, P., Monyer, H., Eds.; Springer: Berlin, 1999; Vol. 141.
6. Conn, P. J.; Pin, J. P. *Ann. Rev. Pharmacol. Toxicol.* **1997**, *37*, 205–237.
7. Arias, R. L.; Tasse, J. R. P.; Bowlby, M. R. *Brain Res.* **1999**, *816*, 299–308.
8. Palmer, G. C. *Curr. Drug Targets* **2001**, *2*, 241–271.
9. Herling, P. L. *Excitatory Amino Acids—Clinical Results with Antagonists*; Academic: London, 1997.
10. Dingledine, R.; Borges, K.; Bowie, D.; Traynelis, S. F. *Pharmacol. Rev.* **1999**, *51*, 7–61.
11. Pellicciari, R.; Costantino, G. *Curr. Opin. Chem. Biol.* **1999**, *3*, 433–440.
12. Monn, J. A.; Valli, M. J.; Massey, S. M.; Wright, R. A.; Salhoff, C. R.; Johnoson, B. G.; Howe, T.; Alt, C. A.; Rhodes, G. A.; Robey, R. L.; Griffey, K. R.; Tizzano, J. P.; Kallman, M. J.; Helton, D. R.; Schoepp, D. D. *J. Med. Chem.* **1997**, *40*, 528–537.
13. Johnson, G.; Ornstein, P. L. *Curr. Pharm. Des.* **1996**, *2*, 331–356.
14. Tikhonova, I. G.; Baskin, I. I.; Palyulin, V. A.; Zefirov, N. S.; Bachurin, S. O. *J. Med. Chem.* **2002**, *45*, 3836–3843, and references cited therein.
15. Hutchison, A. J.; Williams, M.; Angst, C.; De Jesus, R.; Blanchard, L.; Jackson, R. H.; Wilusz, E. J.; Murphy, D. E.; Bernard, P. S.; Schneider, J.; Campbell, T.; Guida, W.; Sills, M. A. *J. Med. Chem.* **1989**, *32*, 2171–2178.
16. Schoepp, D. D.; Jane, D. E.; Monn, J. A. *Neuropharmacology* **1999**, *38*, 1431–1476.
17. Conti, P.; De Amici, M.; De Sarro, G.; Stensbøl, T. B.; Bräuner-Osborne, H.; Madsen, U.; De Micheli, C. *J. Med. Chem.* **1998**, *41*, 3759–3762.
18. Conti, P.; De Amici, M.; Roda, G.; Vistoli, G.; Stensbøl, T. B.; Bräuner-Osborne, H.; Madsen, U.; Toma, L.; De Micheli, C. *Tetrahedron* **2003**, *59*, 1443–1452.
19. Conti, P.; De Amici, M.; Grazioso, G.; Roda, G.; Stensbøl, T. B.; Bräuner-Osborne, H.; Madsen, U.; Toma, L.; De Micheli, C. *Eur. J. Org. Chem.*, **2003**, 4455–4461.
20. Conti, P.; De Amici, M.; Joppolo di Ventimiglia, S.; Stensbøl, T. B.; Madsen, U.; Bräuner-Osborne, H.; Russo, E.; De Sarro, G.; Bruno, G.; De Micheli, C. *J. Med. Chem.* **2003**, *46*, 3102–3108, and references cited therein.
21. De Amici, M.; De Micheli, C.; Gianferrara, T.; Stefancich, G. *Il Farm.* **1997**, *52*, 307–311.
22. Conti, P.; Dallanoce, C.; De Amici, M.; De Micheli, C.; Carrea, G.; Zambianchi, F. *Tetrahedron: Asymmetry* **1998**, *9*, 657–665.
23. Dallanoce, C.; De Amici, M.; Carrea, G.; Secundo, F.; Castellano, S.; De Micheli, C. *Tetrahedron: Asymmetry* **2000**, *11*, 2741–2751.
24. Amori, L.; Costantino, G.; Marinozzi, M.; Pellicciari, R.; Gasparini, F.; Flor, P. J.; Kuhn, R.; Vranesic, I. *Bioorg. Med. Chem. Lett.* **2000**, *10*, 1447–1450.
25. Sih, C. J.; Wu, S.-H. In Eliel, E. L., Wilen, S. H., Eds.; Topics in Stereochemistry; New York: John Wiley, 1989; Vol. 19, pp 63–125.
26. Becke, A. D. *J. Chem. Phys.* **1993**, *98*, 1372–1377.
27. Becke, A. D. *J. Chem. Phys.* **1993**, *98*, 5648–5652.
28. *Ab initio Molecular Orbital Theory*; Hehre, W. J., Radom, L., Schleyer, P. V. R., Pople, J. A., Eds.; John Wiley & Sons, 1986.
29. Cheeseman, J. R.; Frisch, M. J.; Devlin, F. J.; Stephens, P. J. *Chem. Phys. Lett.* **1996**, *252*, 211–220.
30. GAUSSIAN 98, Revision A.3, Frisch, M. J.; Trucks, G. W.; Schlegel, H. B.; Scuseria, G. E.; Robb, M. A.; Cheeseman, J. R.; Zakrzewski, V. G.; Montgomery, Jr., J. A.; Stratmann, R. E.; Burant, J. C.; Dapprich, S.; Millam, J. M.; Daniels, A. D.; Kudin, K. N.; Strain, M. C.; Farkas, O.; Tomasi, J.; Barone, V.; Cossi, M.; Cammi, R.; Mennucci, B.; Pomelli, C.; Adamo, C.; Clifford, S.; Ochterski, J.; Petersson, G. A.; Ayala, P. Y.; Cui, Q.; Morokuma, K.; Malick, D. K.; Rabuck, A. D.; Raghavachari, K.; Foresman, J. B.; Cioslowski, J.; Ortiz, J. V.; Stefanov, B. B.; Liu, G.; Liashenko, A.; Piskorz, P.; Komaromi, I.; Gomperts, R.; Martin, R. L.; Fox, D. J.; Keith, T.; Al-Laham, M. A.; Peng, C. Y.; Nanayakkara, A.; Gonzalez, C.; Challacombe, M.; Gill, P. M. W.; Johnson, B.; Chen, W.; Wong, M. W.; Andres, J. L.; Gonzalez, C.; Head-Gordon, M.; Replogle, E. S.; Pople, J. A. *Gaussian*, Pittsburgh PA, **1998**.
31. Polavarapu, P. L.; Petrovic, A.; Wang, F. *Chirality* **2003**, *15*, S143–S149, **2003**, *15*, 801.
32. Kozikowski, A. P.; Adamczyk, M. *J. Org. Chem.* **1983**, *48*, 366–372.
33. Polavarapu, P. L.; Jiangtao, He. *Anal. Chem.* **2004**, *76*, 61A–67A.
34. Helgaker, T.; Jensen, H. J. A.; Joergensen, P.; Olsen, J.; Ruud, K.; Aagren, H.; Auer, A. A.; Bak, K. L.; Bakken, V.; Christiansen, O.; Coriani, S.; Dahle, P.; Dalskov, E. K.; Enevoldsen, T.; Fernandez, B.; Haettig, C.; Hald, K.; Halkier, A.; Heiberg, H.; Hettema, H.; Jonsson, D.; Kirpekar, S.; Kobayashi, R.; Koch, H.; Mikkelsen, K. V.; Norman, P.; Packer, M. J.; Pedersen, T. B.; Ruden, T. A.; Sanchez, A.; Saue, T.; Sauer, S. P. A.; Schimmelpfennig, B.; Sylvester-Hvid, K. O; Taylor, P. R.; Vahtras, O. *Dalton, a Molecular Electronic Structure Program*, Oslo: University of Oslo, 2001. www.kjemi.uio.no/software/dalton/.